Supporting Information

Chan et al. 10.1073/pnas.1109879108

SI Materials and Methods

Plasmids and Chemicals. Plasmids containing Myr-Akt1-HA under control of the cytomegalovirus promoter were constructed using human or mouse Akt1 cDNA. Mouse AKT1 was fused at the amino-terminus with Src myristoylation signal (Myr, MGSSKSKPKSR) and at the carboxyl-terminus with Hemagglutinin epitope (HA, YPYDVPDYASR) (1). Human AKT1 was fused at the amino-terminus with an extended Src myristylation signal (Myr, MGSSKSKPKDPSQRR) and at the carboxyl-terminus with Hemagglutinin epitope (HA, YPYDVPDYA) (kind gift from D. Defeo-Jones). All mutant constructs of Myr-Akt1-HA were generated using standard molecular biology strategies and were confirmed by DNA sequencing in the core facilities of Kimmel Cancer Center. Green-fluorescence protein (GFP) in pFred143(KH1035) was used in co-transfections to monitor transfection efficiency. HA-epitope-tagged PRAS40 in pRK5 expression vector was from Addgene (#15481). Wortmannin (PI-3 kinase inhibitor), okadiac acid (phosphatase inhibitor), UCN01 [PDK1 inhibitor (2)] and Akt inhibitor VIII [a quinoxaline compound that selectively inhibits Akt1 and Akt2 activity (3, 4)] were purchased from EMD Chemicals. A-443654, an ATP-competitive Akt inhibitor (5), was a kind gift of Abbott Laboratories. ATP and ATP analogs were purchased from Sigma. Phosphatase inhibitor, Calyculin, was from Cell Signaling Technology. Per-VO4 was prepared fresh by mixing equal molar amounts of hydrogen peroxide and NaVO4 (6). Akt-specific substrate peptide (7), RPRAATF, was from Millipore. High affinity I-T15A Akt pseudo substrate peptide, derived from the fusion between an Akt peptide substrate (AKTide-2T) and an Akt substrate peptide from FOXO3 gene (8), (VELDPEFEPRARERAYAFGH), were synthesized by Genscript.

Cell Culture and Transfection. H9C2 cells derived from rat neonatal hearts (ATCC) were cultured in M199 medium supplemented with 10% fetal-calf serum and antibiotics. Human epitheloid carcinoma-derived Hela cells were cultured in Dulbecco's Modified Eagle's Essential Medium (DMEM) supplemented with 10% fetal-calf serum and antibiotics. Cells were transfected using Fugene-6 HD (Roche) according to the manufacturer's protocols. Inhibitors were used on cell culture in the following concentrations: 200 nM wortmannin (PI-3 kinase inhibitor, EMD), 0.5 uM UCN01 (PDK1 inhibitor, EMD), 10 uM VIII (allosteric Akt inhibitor, EMD), 10 uM A-443654 (ATP-competitive Akt inhibitor, Abbott), 100 nM Calyculin A (phosphatase inhibitor, Cell Sign. Tech.) and 250 nM okadiac acid (phosphatase inhibitor, EMD).

In Culture Akt Dephosphorylation. To maximally activate endogenous Akt, H9C2 cells were serum-starved for 4 h before stimulating with 1 ug/mL insulin for 20 min. To initiate dephosphorylation, insulin medium was replaced with serum-free medium in the presence of indicated inhibitors. After 10 min of incubation, cells were harvested for immunoblotting analysis.

Cell Extract Akt Dephosphorylation. Human epitheloid carcinoma-derived Hela cells with Per-VO4 activated Akt (15 min, 100 uM hydrogen peroxide and 100 uM sodium orthovanadate) or expressing Myr-Akt were washed once with ice-cold PBS before placing cell culture dish on an ethanol/dry ice bath to flash freeze. Cell-free extracts were prepared by scraping flash-frozen cells into Phosphatase Assay Buffer (50 mM Hepes, pH 7.5, 100 mM NaCl, 1 mM EDTA, 1 mM EGTA 10 mM NaF supplemented with 5 μg/mL leupeptin, 5 μg/mL aprotinin, 10 mMPMSF, and 1 mMDTT) and then, douncing the extracts with fitted plastic pestle on ice. Total cell-free extracts were incubated at 30 °C to initiate dephosphorylation. The same experiments were performed using serum-starved H9C2 cells stimulated with 1 ug/mL insulin for 20 min.

At the indicated times, a fixed amount of cell extract was removed from incubation and dephosphorylation stopped by adding equal volume of Stop Assay Buffer (25 mM Tris-HCl pH 7.6, 137 mM NaCl, 10% glycerol, 1% NP40, 10 mM NaF supplemented with 5 μg/mL leupeptin, 5 μg/mL aprotinin, 10 mM PMSF, 1 mM NaVO4 and 100 nM Calyculin, 20 mM β-glycerolphosphate and 1 mM Sodium pyrophosphate). After lysis on ice for 10–20 min, phosphatase-inhibited cell lysates was clarified, reduced, and denatured by PAGE sample buffer for immunoblotting.

In Vitro Akt Dephosphorylation by Phosphatase 2A (PP2A). Immunopurified Akt was dephosphorylated in vitro using recombinant PP2A catalytic subunit (PP2A-C). Briefly, Hela cells expressing HA-tagged or Flag-tagged Myr-Akt or maximally phosphorylated wild type (WT)-Akt were lysed in NP40 lysis buffer (25 mM Tris-HCl pH 7.6, 137 mM NaCl, 10% glycerol, 1% NP40, 10 mM NaF) freshly supplemented with 1 mM Sodium pyrophosphate, 5 μg/mL leupeptin, 5 μg/mL aprotinin, 50 nM Calyculin, 1 mM EDTA, 10 mM PMSF,1 mM NaVO4 and 1 mM DTT. For immunoprecipitation, clarified cellular lysates were diluted with equal volume of Phosphatase Assay Buffer (50 mM Hepes, pH 7.5, 100 mM NaCl, 1 mM EDTA, 1 mM EGTA 10 mM NaF supplemented with 5 μg/mL leupeptin, 5 μg/mL aprotinin, 10 mM PMSF, and 1 mM DTT). Akt was immuno-purified by incubation with anti-HA or anti-Flag agarose affinity gel (Sigma) for 3 hours at 4 °C. The immunoprecipitates were washed sequentially at 4 °C, 3× with equal mix of NP40 lysis buffer and Phosphatase Assay Buffer, then, 3× Phosphatase Assay Buffer. After washing, immunoprecipitates were aliquoted and added inhibitors and ATP analogs as indicated at 4 °C. For phospho-Akt in solution experiment, 0.1 ug of recombinant prephosphorylated Akt (Millipore 14–276) was added to each assay.

Dephosphorylation was conducted in Phosphatase Assay Buffer (50 uL final volume, supplemented with 5 mM MgCl2, 30 °C for the indicated times) containing 40 ng recombinant PP2A catalytic subunit (WT or L309 deletion, Cayman Chemicals) and 40 uM 1,2-Dipalmitoyl-*sn*-glycero-3-phosphoserine and 40 uM 1,2-Dipalmitoyl-*sn*-glycero-3-phosphocholine (Echelon Biosciences). After indicated incubation time, assay was stopped by PAGE sample buffer and analyzed for Akt T308 and Akt S473 phosphorylation as well as total Akt and PP2A-C expression.

Immunoblotting. Akt kinase assay and Akt phosphorylation (S473 and T308) were measured as described previously (9). Briefly, cells were homogenized on ice using a NP40 lysis buffer (25 mM Tris-HCl pH 7.6, 137 mM NaCl, 10% glycerol, 1% NP40, 10 mM NaF) freshly supplemented with 1 mM Sodium pyrophosphate, 5 μg/mL leupeptin, 5 μg/mL aprotinin, 1 mM EDTA, 10 mM PMSF,1 mM NaVO4 and 1 mM DTT. Clarified cellular lysates were boiled and separated by electrophoresis in a 4–12% SDS-PAGE and transferred onto nitrocellulose membranes. For immunoblotting, membranes were blocked for 30 min with Li-Cor blocking buffer and probed with antibodies at 4 °C overnight. The blots were subsequently incubated with either IRDye 700 or 800 secondary antibodies conjugated with infrared fluorophores for 60 min. Bands were visualized and directly quantified using the Odyssey Infrared Imaging System (Li-Cor, Lincoln, NE). The following antibodies were used at 1:1,000 dilution: antiphospho-

GSK3 (Ser21/9), antiphospho-Pras40 (Ser246), antiphospho Erk1/2, antitotal Akt, antiphospho-Akt (T308), antiphospho-Akt (S473), anticleaved Caspase-3 (Asp175) (5A1E) and antitotal Caspase-3 (from Cell Signaling Tech.), antiGAPDH (from Santa Cruz) and antiHA (from Covance).

Immunofluorescence Microscopy. Immunofluorescence microscopy procedures and image acquisition were performed as previously described (10). Briefly, H9C2 cells were plated onto glass cover slips and transiently transfected with plasmids using Fugene HD. After 24 h, cells were fixed with PBS containing 4% paraformaldehyde and 100 mM EGTA for 20 min. Fixed cells were made permeable by incubating with blocking buffer (0.01M Tris-HCl, PH 7.5, 0.15 M NaCl, 0.1% BSA and 0.002% NaN3) containing 0.2% Triton X-100 for 5 min at room temperature. Subsequently, the cover slips were incubated with antiHA (Covance) and antiphospho-Akt (T308) (Cell Signaling Tech) antibodies in a 37 °C-humidified incubator for 45 min. After rinsing with blocking buffer, the myocytes were incubated with Alexa-594 and Alexa-488 conjugated secondary antibodies (1:2,000) and 350 nM DAPI nuclear stain. After incubation and washing, the cover slips were mounted and sealed with ProLong Gold reagent (Invitrogen) and stored in the dark at 2–6 °C. Images were taken with a Confocal Microscope (Zeiss LSM 510 META Confocal, KCC Bioimaging facility).

Cell Fractionation. Cytosol and total cell membranes were prepared using an Extraction Kit (Biovision). Briefly, plasmids were transiently transfected in H9C2 cells for forty-eight h. Cells were collected by scraping in PBS and then pelleted (3,000 rpm for 5 min). Cells were resuspended in the provided Homogenize Buffer and homogenized. The homogenate were centrifuged in $700 \times g$ at 4 °C for 10 min to collect supernatant. The collected supernatant was centrifuged at high speed ($10{,}000 \times g$, 30 min, 4 °C) to yield total cellular membrane (pellet) and cytosol.

Modeling Structure. Structural figures were prepared using PyMOL based on structures of activated Akt2 with AMP-PNP/Mg^{2+} or with A446534 (11, 12).

Protease Cleavage-Based Fluorescent Cell Viability Assay. Viability of H9C2 cells expressing Akt mutants was determined by cleavage activities of live-cell-dependent proteases using the cell-permeable fluorogenic peptide substrate, GF-AFC (Promega) as described (13). GF-AFC cannot be cleaved upon loss of cell membrane integrity or by necrotic and apoptotic cell activated proteases. Briefly, H9C2 cells were transfected with indicated plasmids without cotransfecting GFP plasmids tracers to avoid fluorescent interference. After 24 to 36 h, cells were trypsinized and replated onto black-walled, clear bottom 96 well plates (20,000 cells/well). After 6 h, cell medium was changed to either 10% fetal-calf serum medium, 1% fetal-calf serum medium, or 0.5 uM staurosporine medium. After 12–13 h of incubation, cell viability was determined by adding GF-AFC peptide substrates at 37 °C for 30 min. Fluorescence was measured using a BioTek multimode fluorometer/luminometer.

In Vitro Akt Kinase Assay. In vitro Akt/PKB kinase activation was determined by the phosphorylation of the recombinant Gsk3 peptide substrate as described by the manufacture (Cell Signaling Technology). Phosphorylated GSK3-peptide was visualized and quantified by anti-phospho-GSK3.

Molecular Dynamics Stimulation. The program CHARMM (Chemistry at HARvard Molecular Mechanics) was used for all-atom modeling and molecular dynamics (14). The CHARMM force field, originally parameterized by Momany and Rone has been extended to describe ligands in the Ligand-Protein Database (LPDB) (15), and was used to build potential energy functions for modeled complexes of Akt with ADP and ATP. The ATP and ADP complex was modeled into the crystal structure of AKT kinase bound to AMP-PNP (1o6k) which is very similar in structure to PKA complexes of ADP/ATP (1rdq) and ADP-Mg-F_3 (1l3r).

All-atom molecular modeling and molecular dynamics (MD) simulations were performed to investigate the stability of the modeled ATP and ADP conformations both with and without the two bound catalytic Mg^{2+} ions. In flexible receptor CHARMM-based molecular docking, short molecular dynamics simulations using implicit solvent are used to assess the geometry and the stability of top-ranked protein-ligand complexes, in order to determine the most stable dynamic conformation of the native complex (16). This procedure is used to compare the differences in the dynamics of the ATP and ADP bound conformation of Akt and follow changes in the H194 and pT308 interaction. In these short MD simulations, the electrostatic contribution to the solvation energy is approximated by using the generalized Born implicit solvent potential energy term (GBMV) (17).The all-atom complexes were first minimized for 500 steps using the standard all-atom potential function with a distance dependent dielectric, and then an additional 500 steps using the GBMV implicit solvent. MD simulations are performed using a 16 Å nonbonded cutoff and with GBMV implicit solvent for 10,000 (1 fs) steps. Differences in the stability of the H194 and pT308 interaction between the ADP and ATP bound states in simulations at 300 K were also verified by duplicate trajectories and a temperature titration of duplicate trajectories at multiple temperatures (300, 400, 500, 600, 700, 800, 900, 1,000 K).

1. Bellacosa A, et al. (1998) Akt activation by growth factors is a multiple-step process: the role of the PH domain. *Oncogene* 17:313–325.
2. Sato S, Fujita N, Tsuruo T (2002) Interference with PDK1-Akt survival signaling pathway by UCN-01 (7-hydroxystaurosporine). *Oncogene* 21:1727–1738.
3. Barnett SF, et al. (2005) Identification and characterization of pleckstrin-homology-domain-dependent and isoenzyme-specific Akt inhibitors. *Biochem J* 385:399–408.
4. Logie L, et al. (2007) Characterization of a protein kinase B inhibitor in vitro and in insulin-treated liver cells. *Diabetes* 56:2218–2227.
5. Luo Y, et al. (2005) Potent and selective inhibitors of Akt kinases slow the progress of tumors in vivo. *Mol Cancer Ther* 4:977–986.
6. Bennett PA, Dixon RJ, Kellie S (1993) The phosphotyrosine phosphatase inhibitor vanadyl hydroperoxide induces morphological alterations, cytoskeletal rearrangements and increased adhesiveness in rat neutrophil leucocytes. *J Cell Sci* 106:891–901.
7. Bozinovski S, Cristiano BE, Marmy-Conus N, Pearson RB (2002) The synthetic peptide RPRAATF allows specific assay of Akt activity in cell lysates. *Anal Biochem* 305:32–39.
8. Luo Y, et al. (2004) Pseudosubstrate peptides inhibit Akt and induce cell growth inhibition. *Biochemistry* 43:1254–1263.
9. Chan TO, et al. (2002) Small GTPases and tyrosine kinases coregulate a molecular switch in the phosphoinositide 3-kinase regulatory subunit. *Cancer Cell* 1:181–191.
10. Chan TO, et al. (2008) Cardiac-restricted overexpression of the A_{2A}-adenosine receptor in FVB mice transiently increases contractile performance and rescues the heart failure phenotype in mice overexpressing the A_1-adenosine receptor. *Clinical and Translational Science* 1:126–133.
11. Davies TG, et al. (2007) A structural comparison of inhibitor binding to PKB, PKA and PKA-PKB chimera. *J Mol Biol* 367:882–894.
12. Yang J, et al. (2002) Crystal structure of an activated Akt/protein kinase B ternary complex with GSK3-peptide and AMP-PNP. *Nat Struct Biol* 9:940–944.
13. Niles AL, et al. (2007) A homogeneous assay to measure live and dead cells in the same sample by detecting different protease markers. *Anal Biochem* 366:197–206.
14. Brooks BR, et al. (2009) CHARMM: the biomolecular simulation program. *J Comput Chem* 30:1545–1614.
15. Roche O, Kiyama R, Brooks CL, 3rd (2001) Ligand-protein database: linking protein-ligand complex structures to binding data. *J Med Chem* 44:3592–3598.
16. Armen RS, Chen J, Brooks CL, 3rd (2009) An evaluation of explicit receptor flexibility in molecular docking using molecular dynamics and torsion angle molecular dynamics. *J Chem Theory Comput* 5:2909–2923.
17. Feig M, et al. (2004) Performance comparison of generalized born and Poisson methods in the calculation of electrostatic solvation energies for protein structures. *J Comput Chem* 25:265–284.

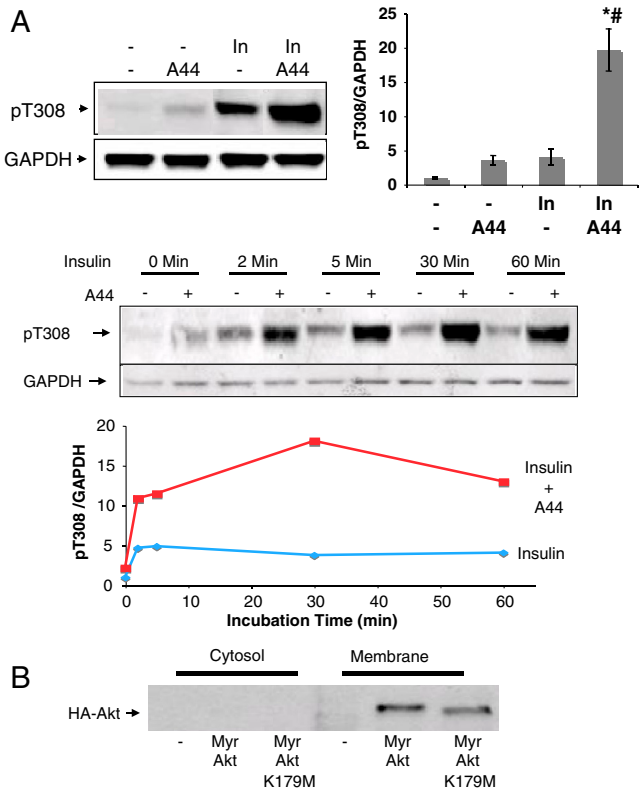

Fig. S1. (*A*) A-443654 synergized with insulin to induce Akt hyperphosphorylation. H9C2 cells were serum-starved for 4 h and stimulated with 1 ug/mL insulin for the time indicated in the presence or absence of 4 uM A-443654. Representative immunoblots of phospho-T308 and GAPDH in serum-starved H9C2 cells treated with A-443654 and/or insulin. Graph shows quantification of phospho-T308/GAPDH ratio at 15 min time point from 3–7 independent experiments/group: mean + / – SE. *$p < 0.05$ vs. insulin, #$p < 0.05$ vs. A-443654. (*B*) Myr-Akt1 and Myr-Akt1 K179M plasmids were transiently transfected in H9C2 cells for 48 h. Cytosol and total cell membranes were prepared using a membrane extraction kit (Biovision) and immunoblotted with antiHA antibody.

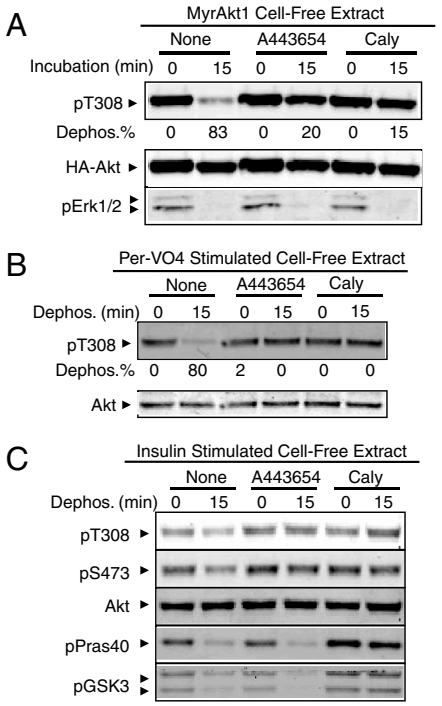

Fig. S2. (*A*) Myr-Akt1 plasmid was transiently expressed in Hela cells for 48 h and was then flash-frozen. Aliquots of cell extracts were added with A443654 or calyculin on ice before incubation at 30 °C for 15 min. Cell extracts were analyzed for Akt Thr308 phosphorylation, Erk 1 and 2 phosphorylation, total Akt and GAPDH by immunoblotting. Quantification shows the percentage of Akt dephosphorylation (Dephos. %) relative to maximal Akt phosphorylation. (*B*) To phosphorylate endogenous Akt in Hela cells, cells were stimulated with 100 uM Per-VO4 for 15 min and snap-frozen using an ethanol-dry ice bath. Cell extracts were treated with 10 uM A-443654 (A44) or 100 nM calyculin (Caly) at 4 °C before incubating at 30 °C for 15 min. Quantification shows the percentage of Akt dephosphorylation (Dephos. %) relative to maximal Akt phosphorylation. (*C*) H9C2 cells were stimulated with insulin to maximally phosphorylate Akt before snap-freezing. Ice-cold cell extracts were added with 10 uM A-443654 (A44) or 100 nM calyculin (Caly) before incubating at 30 °C for 15 min. After incubation, protein extracts were subjected to immunoblot analysis using antibodies detecting phosphorylated Akt (T308 or S473), GSK3β (S9), and PRAS40 (T246). Quantification shows the percentage of Akt dephosphorylation (Dephos. %) relative to maximal Akt phosphorylation.

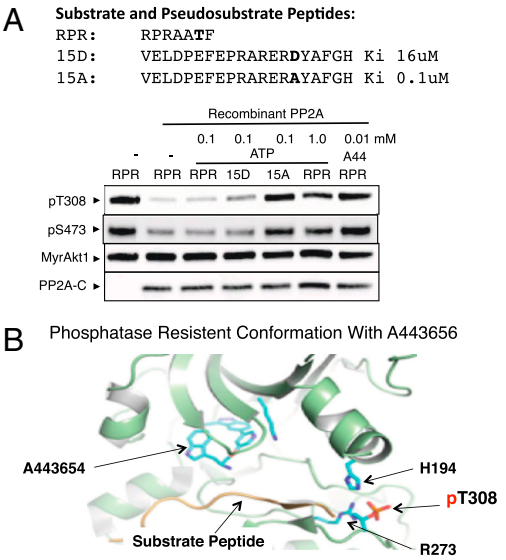

Fig. S3. (*A*) ATP, but not A443654, required pseudosubstrate inhibitor peptide to block Akt dephosphorylation. Top: amino acid sequences of Akt substrate peptide (RPR) and pseudosubstrate peptide inhibitors (15 D and 15 A) and Ki values are depicted. Experiments showed immunoprecipitated phospho-Myr-Akt1 was incubated with recombinant PP2A and 5 mM $MgCl_2$ for 30 min, 30 °C in the presence of A443654, ATP, and peptides as indicated. Myr-Akt1 T308/S473 phosphorylation, HA-tagged Myr-Akt1 and PP2A-C expression are shown. (*B*) Based on X-ray crystal structure (11), schematic depiction of Akt1 nucleotide binding pocket containing the ATP-competitive inhibitor, A-443654 in which phosphorylated T308 interacts with amino acids H194 and R273. The depicted structure illustration is modeled on active human Akt2 crystal structure (PDB 2jdr) bound with A-443654. However, we denoted ATP and Mg^{2+} and corresponding Akt1 amino acid residues for clarity.

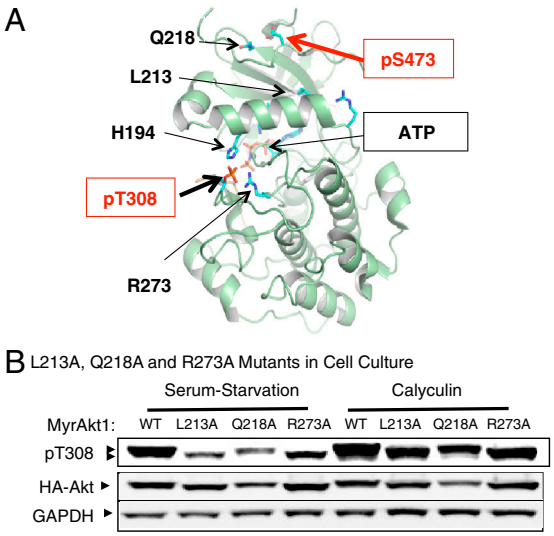

Fig. S4. Mutating Akt1 L213 and Q218 enhances Myr-Akt1 dephosporylation. (*A*) Akt1 catalytic cleft drawing showing the nucleotide binding pocket with bound ATP and phosphorylated-T308, H194, R273, phosphorylated-S473, L213, Q218 residues (12). The depicted structure illustration is modeled on active human Akt2 crystal structures bound to ATP analog AMP-PNP and Mn^{2+} (PDB 1o6k). However, we denoted ATP and Mg^{2+} and corresponding Akt1 amino acid residues for clarity. Also, pS473 is represented by a phosphomimic (S473D). (*B*) MyrAkt1 L213A and Q218A mutants were transfected into Hela cells. After 48 h, cells were propagated for four additional hours in exogenous growth factor-free medium followed by adding calyculin phosphatase inhibitor and insulin for 15 min. Akt T308, HA-tag and GAPDH were analyzed by immunoblotting.

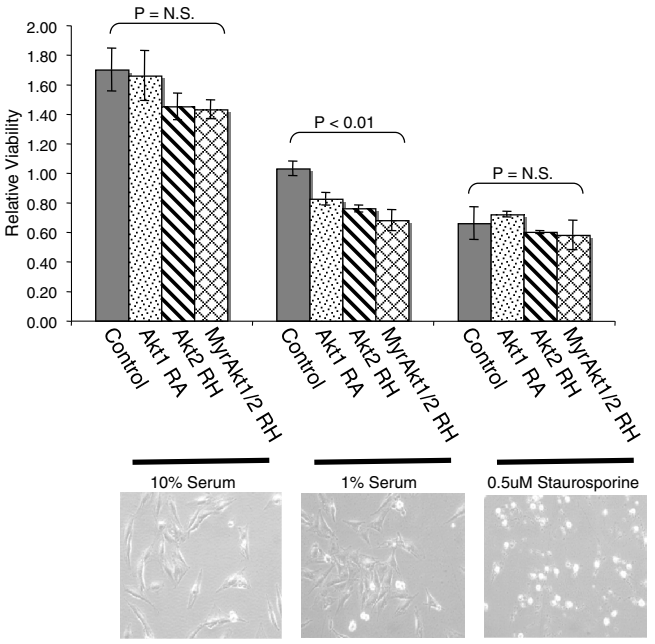

Fig. S5. Cell viability assay. Akt1-R273A, Akt2-R274H, MyrAkt1-R273H, and MyrAkt2-R274H were transfected into H9C2 cells in the indicated combinations. After 24 h, cells were trypsinized and replated onto 96 well plates for 6 h. Then, cell culture medium were changed to contain either 10% FBS, 1% FBS and 0.5 uM staurosporine as indicated for 12–13 h. Cell viability was determined by adding the cell-permeable fluorogenic peptide substrate, GF-AFC. The graph shows viability normalized to cells transfected with control plasmids in 1% FBS culture medium. Bracketed numbers indicate the number of repeats from two to three independent experiments. Values were analyzed by nonparametric ANOVA (Kruskal-Wallis with Dunn posttest). Pictographs show phase contrast images of H9C2 cells transfected with control plasmids under different growth conditions.

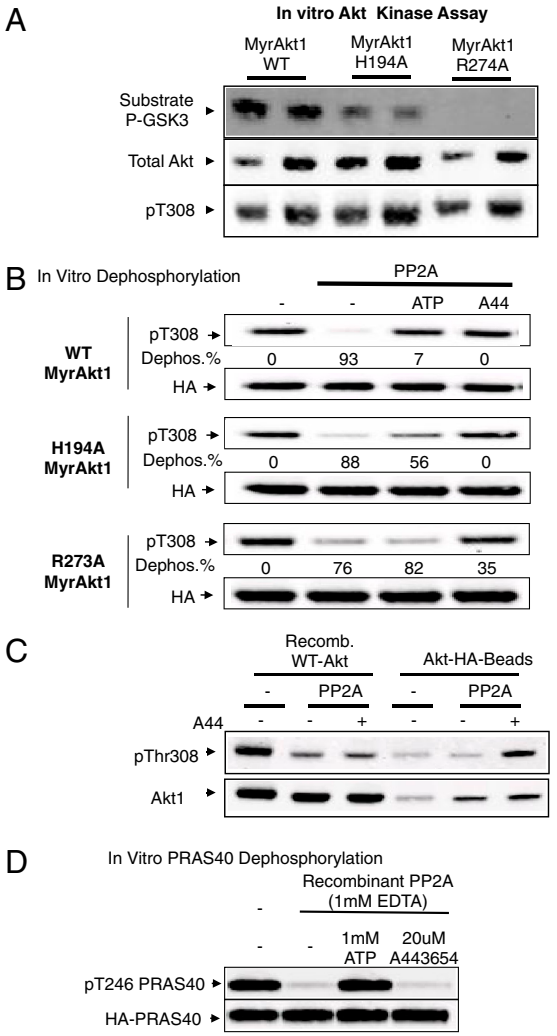

Fig. S6. (*A*) MyrAkt1 R273A is catalytically inactive. MyrAkt1 WT and R273A mutant were expressed in Hela cells and prephosphorylated by incubation with 1 ug/mL insulin and 50 nM phosphatase inhibitor, calyculin for 20 min. Akt proteins were immunoprecipitated from cell extracts and incubated with GSK3 recombinant substrate peptide and kinase assay buffer for 5 min at room temperature. Phosphorylation was determined by antiphospho-specific antibodies. (*B*) Cells expressing H194A or R273A Myr-Akt mutants were maximally phosphorylated by incubation with 1 ug/mL of insulin and 50 nM calyculin phosphatase inhibitor for 20 min. Then immuno-purified Myr-Akt1 mutants were incubated with recombinant PP2A-C in the presence of 25 uM I-T15A peptide, 5 mMMgCl2, 0.1 mMATP, or 10 uM A443654 and then, analyzed for Akt phosphorylation (T308) and HA-tag by immunoblotting. Quantification shows the percentage of Akt dephosphorylation (Dephos. %) relative to maximal Akt phosphorylation. (*C*) A443654 failed to block the dephosphorylation of Akt in solution. 0.1 ug of recombinant prephosphorylated phospho-Akt1 in solution or immunoprecipitated phospho-Akt1 was incubated with recombinant PP2A for 30 min, 30 °C in the presence of 10 uM A443654. Immunoblot images show Akt T308 phosphorylation and Akt1 expression. (*D*) Without $MgCl_2$, 1 mM ATP, but not 20 uM A-443654, directly inhibits PP2A catalytic activity. Hela cells expressing HA-tagged PRAS40 were stimulated with 100 uM Per-VO4 for 15 min to induce PRAS40 phosphorylation. Then, phospho-PRAS40 were immuno-purified and dephosphorylated by recombinant PP2A in a buffer with 1 mM EDTA. 1 mM ATP or 20 uM A-443654 were added as indicated. Immunoblots shows PRAS40 (Thr246) phosphorylation and total PRAS40 expression.